Biochimica et Biophysica Acta 1838 (2014) 2530–2538

Contents lists available at ScienceDirect

Biochimica et Biophysica Acta

journal homepage: www.elsevier.com/locate/bbamem

Interactions of pentacyclic triterpene acids with cardiolipins and related phosphatidylglycerols in model systems

Marcin Broniatowski *, Michał Flasiński, Katarzyna Zięba, Paweł Miśkowiec

Department of Environmental Chemistry, Faculty of Chemistry, Jagiellonian University, Gronostajowa 3, 30-387 Kraków, Poland

ARTICLE INFO

Article history:
Received 21 March 2014
Received in revised form 23 May 2014
Accepted 27 May 2014
Available online 4 June 2014

Keywords:
Pentacyclic triterpene acid
Langmuir monolayer
Cardiolipin
Phosphatidylglycerol

ABSTRACT

Pentacyclic triterpene acids (PTAs): betulinic (BAc), oleanolic (Ola) and ursolic (Urs) are potent pharmaceuticals applied in the therapy of cancer and bacterial infections. The mechanism of PTA action is multifactor, but the important step is their interaction with the lipids of mitochondrial and bacterial membranes. In our studies we applied the Langmuir monolayer technique to investigate the interactions between PTAs and cardiolipins (CLs) and phosphatidylglycerols (PGs). We applied two different mammalian mitochondrial CLs and one species extracted from the membrane of *Escherichia coli*. For comparison we performed the same experiments on the systems containing PTAs and 3 PGs strictly correlated structurally to the applied CLs. Our studies proved that PTAs can disturb the organization of CL-rich domains and affect the bacterial membrane fluidity by the interactions with phosphatidylglycerols, so anionic phospholipids are the targets of their membrane action. The thermodynamic interpretation of the results indicated that Urs has the highest membrane disorganizing potential among the 3 studied PTAs. The studies performed on model systems proved also that BAc can discriminate over structurally similar animal cardiolipin species, interacts specifically with BHCL — the main mammalian CL and can disturb its organization in the membrane. In contrast, Ola and Urs are much active as far as the interaction with bacterial CLs and PGs is concerned.

1. Introduction

Betulinic (BAc), oleanolic (Ola) and ursolic (Urs) acids are isomeric pentacyclic triterpene carboxylic acids (PTAs) of high pharmacological potential, which are isolated worldwide from different medicinal plants used in folk medicine [1–3]. The structures of these bioactive PTAs are summarized in Scheme 1.

As it is visible, PTAs are isomers which differ only in the structure of the last E ring. In BAc the ring E is five-membered and the carbon atoms C20, C29 and C30 are shifted to the isopropene substituent. In Ola and Urs ring E is six-membered cyclohexane. Ola and Urs differ in the location of the C30 carbon atom (CH_3 group). Additionally, in BAc all the rings are *trans*-fused leading to their coplanar location, whereas in Ola and Urs the junction between D and E rings is *cis* leading to the distortion of the E ring from the plane defined by A–D rings [4].

BAc, Ola and Urs are intensively investigated because of their multiple pharmaceutical activities combined with relatively low toxicity to normal eukaryotic cells. The most important here are the anticancer and chemopreventive properties [5–9]. Generally, PTAs are able to induce apoptosis of cancer cells on the mitochondrial pathway [10–13]. The mechanism of their action is not exactly elucidated but it is believed that their incorporation into mitochondria triggers the generation of reactive oxygen species (ROS) leading to the peroxidation of some mitochondrial membrane phospholipids and the following permeation [14]. The leak of mitochondrial complexes like cytochromes into the cytosol activates the caspase cascades leading finally to apoptosis. Taking into consideration the number of scientific papers, the next in the order of importance is the antimicrobial activity of PTAs [15,16]. Indeed, they proved to be bactericides both against Gram-positive and Gram-negative bacterial strains, and what should be here underlined, in some cases they were also active against bacterial strains exhibiting multidrug resistance [17,18]. PTAs were also promising antiviral substances, especially in HIV infections [19,20]. PTAs were also tested as drugs against diseases of different etiology from inflammation treatment [21], via obesity prevention [22] to Alzheimer disease therapy [23], to mention only some extremes of the research.

The described PTAs here differ significantly in their pharmaceutical potential, depending on the area of the research. In the field of anticancer therapy BAc turned out to be the most active and most versatile of them [8]. However, as far as the antibacterial activity is concerned, BAc is considered inactive in most of the performed studies in contrast

* Corresponding author. Tel.: +48 126646795; fax: +48 126340515.
E-mail address: broniato@chemia.uj.edu.pl (M. Broniatowski).

http://dx.doi.org/10.1016/j.bbamem.2014.05.027
0005-2736/

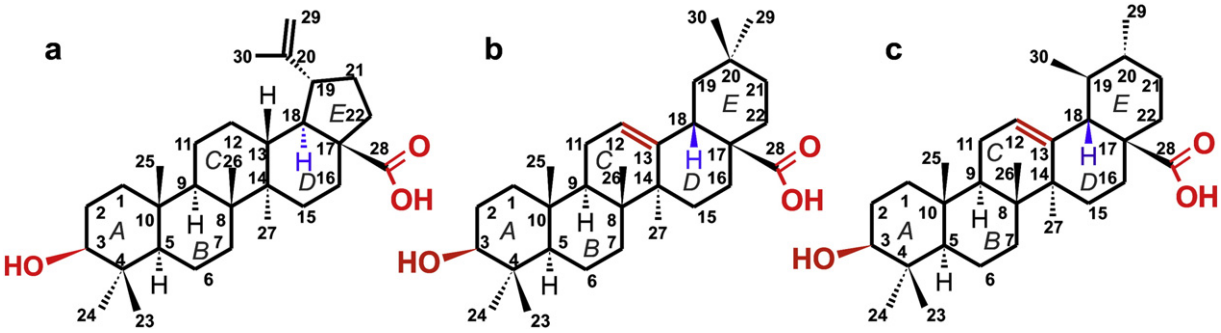

Scheme 1. Structural formulas of: a) BAc, b) Ola, and c) Urs. Black — skeletons of the ground triterpene alkanes: a) lupane, b) oleanane, and c) ursane. Red — polar groups and the additional double bond in ring C of Ola and Urs. Blue — the important chiral center on the ring D–ring E junction.

to isomers Ola and Urs [16]. Regarding Ola and Urs, they also differ mutually in their activity depending on the particular case. PTAs are surface active compounds which are structurally similar to steroids, originating also from squalene [24]. Therefore, their interactions with mitochondrial and bacterial membranes can be the crucial step in the mechanism of their action [25,26]. The hypothesis claiming that mitochondria evolved from bacteria is widely accepted, and one of the arguments of its supporters is the presence of unique phospholipids in the membranes of both mitochondria and bacteria [27]. These unique phospholipids which do not occur in normal cellular membranes are cardiolipins — dimeric phosphatidylglycerol molecules possessing 4 acyl chains bound to one head-group [28–30].

Mitochondrial and bacterial membranes are complicated multicomponent systems; therefore the reductive approach is here necessary and appropriate model environment should be applied. In our preliminary studies we do not intend to model the membranes but to investigate the interactions of the terpenes with cardiolipins and phosphatidylglycerols in simplified binary systems. To achieve this aim we applied Langmuir monolayers formed by these substances at the air/water interface as the versatile platforms enabling such investigation. Although Langmuir monolayers can be considered extremely artificial compared to real biomembranes, numerous studies regarding the interactions of various membrane active drugs with membrane phospholipids were performed with their application providing valuable results. The Langmuir monolayer technique is beneficial in some aspects compared with other membrane mimicking systems: the composition of the monolayer and the number of film forming molecules are strictly controlled, while by the film compression that required organization of the molecules can be achieved [31].

In our studies we applied three different cardiolipins: BHCL — tetralinoleoyl CL, the cardiolipin species most populated in mammalian mitochondria, TOCL — tetraoleoyl CL, the cardiolipin dominating in human lymphoblasts and ECCL — bacterial CL extracted from *Escherichia coli*. Cardiolipins are not the only anionic phospholipids present in bacterial membranes. They are accompanied by phosphatidylglycerols (PGs) [32]. Therefore, in our studies we also investigated binary monolayers formed by the three PTAs and three different PGs. The PGs were selected in such a way that the investigated cardiolipins can be considered dimers of the particular PGs. Such an approach enabled us the comparison of the interactions of PTAs with CLs and PGs and the elucidation of the question which of the anionic phospholipids is targeted by the PTAs in bacterial membrane: CLs or PGs? In our studies we recorded surface pressure (π)–mean molecular area (A) isotherms for different compositions of the binary film. This technique was combined with the visualization of the investigated monolayers by Brewster angle microscopy (BAM). We also performed thermodynamic analysis of the registered data, calculating the excess functions of mixing. The combination of these methods enabled the thorough characterization of the interactions of anionic membrane phospholipids with the bioactive PTAs in the model environment.

2. Experimental

2.1. Materials

Betulinic acid (98%), oleanolic acid (99%) and ursolic acid (99%) were purchased from Sigma Aldrich. All the phospholipids were supplied by Avanti Polar Lipids. We bought 6 anionic lipids in the form of lyophilized powders of high (>99%) purity. There were: beef heart CL (BHCL, tetralinoleoyl CL) extracted from the beef heart, tetraoleoyl CL (TOCL, synthetic sample), cardiolipin extracted from *E. coli* (ECCL), dilinoleoyl PG (DLPG, synthetic sample), dioleoyl PG (DOPG, synthetic sample) and the PG extracted from *E. coli* (ECPG). The exact names and structures of the investigated compounds as well as the information about the fatty acid distribution can be found in Supplementary materials and on the producer's website [33]. For the preparation of solutions we applied HPLC grade chloroform (99%) stabilized by ethanol and HPLC grade methanol (99.9%). As the subphase ultrapure water of the resistivity 18.2 MΩ·cm was applied, the ultrapure water was produced on site with the Millipore Synergy system.

2.2. Solutions

The investigated PTAs and anionic phospholipids were dissolved in chloroform/methanol 9/1 v/v mixture. The concentrations of the solutions oscillated between 0.2 and 0.3 mg/ml, which gives PTA molar concentrations from 4.4 to $6.6 \cdot 10^{-4}$ M, ca. 1.3 to $2.0 \cdot 10^{-4}$ M for CLs and from 2.7 to $4.0 \cdot 10^{-4}$ M for PGs. The binary mixtures were prepared from the stock solutions in darkened glass vials just before the given experiment. In this paper we present the data for 18 binary systems (6 phospholipids combined with 3 terpenes). The applied surfactants differ in the cross section, thus it was preferable to keep constant surface proportions of the molecules and not mole ratios. For each of the 18 binary systems we investigated 5 different surface proportions of the surfactants (terpene: phospholipid): 1:4, 1:2, 1:1, 2:1, and 4:1. In Supplementary materials the problem of the recalculation of the surface proportions into mole ratios is covered in details.

2.3. Langmuir technique

In our experiments we used a KSV (KSV, Helsinki, Finland) double-barrier Langmuir trough with nominal area of 273 cm^2. BAM experiments were performed on a larger instrument with an area of 840 cm^2 designated by KSV for microscopic experiments. Surface pressure was monitored with a Wilhelmy-type tensiometer with a filtration paper strap (Whatman, ashless) as the pressure sensor. Surface pressure was acquired with a 1 s time log and every π value is an average of 5 single measurements. The accuracy of the sensor was 0.1 mN/m.

Before an experiment the Langmuir trough was carefully cleaned, after which it was filled with ultrapure water. The appropriate volume of the chloroform/methanol solution of investigated surfactant(s) was

deposited at the water/air interface with a Hamilton microsyringe. 5 min were left for the spreading solvent evaporation, after which the monolayers were compressed with the barrier speed of 20 cm^2/min. All the π–A isotherms were registered at least three times (the experimental error did not exceed 1 $Å^2$) and the average curves were taken for the calculation of the thermodynamic functions. The subphase temperature was 20 ± 0.1 °C in all the experiments and was controlled by Julabo water circulating bath.

2.4. Calculations

Compression modulus C_S^{-1} was calculated according to its definition: $C_S^{-1} = -A d\pi / dA$.

The excess free energy of mixing was calculated according to its definition [34]:

$$\Delta G^{exc} = \int_0^{\pi} A^{exc} d\pi$$

where A^{exc} is the excess area defined as follows:

$$A^{exc} = A_{12} - (A_1 X_1 - A_2 X_2)$$

where A_{12} is the mean molecular area at a given π value for the binary monolayer, A_1 is the molecular area at the same π for the surfactant1 (one component) monolayer, and A_2 is the molecular area at the same π value for the surfactant2 (one component) monolayer. X_1 and X_2 are mole ratios of surfactant1 and surfactant2 in the binary monolayer ($X_1 + X_2 = 1$).

2.5. Brewster angle microscopy

Brewster angle microscopy experiments were performed with an UltraBAM instrument (Accurion GmbH, Goettingen, Germany) equipped with a 50 mW laser emitting p-polarized light at a wavelength of 658 nm, a 10× magnification objective, a polarizer, an analyzer and a CCD camera. The spatial resolution of the BAM was 2 μm. The instrument was coupled with the KSV 2000 Langmuir trough and installed on an antivibration table.

3. Results

The article concerns mixed binary systems; however, it would be reasonable to start from a short description of one-component monolayers formed by the investigated chemicals. The monolayers of the six investigated anionic lipids have an expanded character and their state can be characterized as liquid expanded (LE). The π–A isotherms and C_S^{-1}–π curves are shown in Supplementary materials. The monolayers of the investigated anionic phospholipids were visualized with the application of the BAM technique; however, as it is typical for the LE state, the monolayers were homogenous within the whole range of compression. Regarding the PTAs, the monolayers of Urs have not been characterized in the last decades, whereas the data regarding BAc and Ola are scattered in the literature [35,36]. Therefore, it was reasonable to summarize the characteristics of the monolayers together. Fig. 1 shows the π–A isotherms, C_S^{-1}–π dependences and representative BAM images for these three compounds.

The π–A isotherms of the three investigated PTAs have similar characteristics. The slow rise of the surface pressure starts at ca. 80 $Å^2$ and at ca. 60 $Å^2$ a rapid rise of surface pressure can be observed in the course of the isotherms. The monolayers are very stiff and the Wilhelmy plate can be deformed during the compression [36] which can result in lower reproducibility of the isotherms, especially as the value of the collapse pressure is concerned. The values of C_S^{-1} are rather low and hardly achieve the limit of 100 mN/m. Thus, the interpretation of C_S^{-1}–π dependence can lead to the misleading conclusion that the monolayers are in the liquid expanded state. The wrongness of such an interpretation is proved by the BAM images. The BAM photos of the monolayers of the three terpenes are mutually similar. At first glance they are heterogeneous as brighter domains with sharp edges can be observed on a black background. The acids are bolaamphiphilic; but their stiff skeleton of fused cycloalkane rings cannot be bent, so they cannot achieve the U-shaped conformation at the water/air interface [37]. As it was proved in the scientific literature, the packing abilities of triterpene acids in monolayers depend on the orientation of the molecules at the interface. If the –OH group is in contact with water, the molecules are oriented perpendicularly and can form crystalline domains of solid character [35]. On the contrary, when the –COOH group is in contact with water, the molecules are tilted in the monolayer, the domains formed by them are amorphous, and the state of such domains is liquid expanded. Both orientations coexist in monolayers;

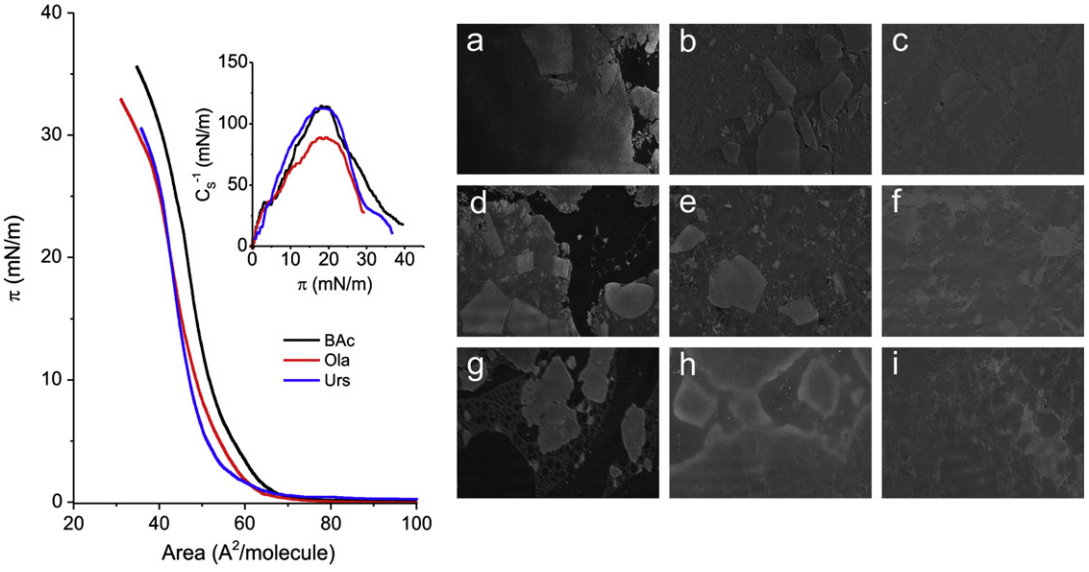

Fig. 1. Left, π–A isotherms and C_S^{-1}–π curves (inset) for the investigated triterpene acids. Right, representative BAM images. a–c) BAc, d–f) Ola, and g–i) Urs; a, d, g – π = 2 mN/m; b, e, h – π = 10 mN/m; c, f, i – π = 20 mN/m.

therefore, the films are so heterogeneous. Upon the compression some molecules are switched from their tilted to upright orientation and the condensed crystalline domains dominate in the monolayer; however, even at high surface pressures the monolayers are not fully homogeneous.

3.1. Interactions of triterpene acids with cardiolipins

For the studies of the interactions of PTAs with cardiolipins three different terpene acids and three cardiolipins were applied which gives 9 binary systems, which were investigated. In each system 5 different proportions of the components were investigated as it is described in the Experimental section. The registered π–A isotherms and calculated C_S^{-1}–π dependences are shown in Supplementary materials. On the basis of the measured π–A isotherms thermodynamic analysis was performed and the calculated excess free energy of mixing (ΔG^{exc})–X(terpene) plots are gathered in Fig. 2.

As it is visible in Fig. 2 the interactions between PTAs and CLs expressed in the form of ΔG^{exc}–X(terpene) plots strongly depend on the applied terpene. In all three systems with Urs ΔG^{exc} acquires positive sign and the values are relatively high. The highest values are observed in the system Urs/TOCL, whereas in the systems of Urs/BHCL and Urs/ECCL, for higher Urs proportions, ΔG^{exc} values are close to 0. In the systems with Ola and BAc ΔG^{exc} values are close to 0 or negative. Only in the system BAc/BHCL positive values can be noticed for lower BAc ratios. On the other hand, only BAc can be treated as a terpene which discriminates over the CLs, as in all systems with Urs the ΔG^{exc} values are positive and in systems with Ola close to 0 or slightly negative. The most striking observation is the discrimination over the tetralinoleoyl (BHCL) and tetraoleoyl (TOCL) cardiolipins manifested by BAc. In the system BAc/BHCL ΔG^{exc} values are positive for lower BAc proportions and close to 0 for higher proportions, whereas in the system BAc/TOCL all ΔG^{exc} values are significantly negative.

For the better characterization of the investigated systems collapse pressures and maximal C_S^{-1} values were drawn against the terpene mole ratio and such plots are presented in Fig. 3.

As far as the π_{coll}–X(terpene) plots are considered, the systems with BAc differ profoundly from the systems with Ola and Urs. π_{coll} falls here quite linearly with increasing X(terpene). On the contrary, the collapse pressures in the systems with Urs are on a constant level regardless of X(terpene) or even slowly growing with the increasing X(terpene) in the system with Ola. For immiscible monolayers two collapse pressures typical for pure components are observed upon compression, whereas for miscible films one collapse pressure depending on the composition is expected [34]. In our case there are no two separate collapses, so the π_{coll}–X(terpene) plots corroborate mutual miscibility in the systems. The systems with BAc behave in a way which can be predicted for typical miscible films — π_{coll} decreases linearly from the highest value observed for CLs to the lowest value observed for BAc. The situation for the systems with Ola and Urs is different — there is only one collapse pressure observed, which is higher than the collapse pressures of both components. Such behavior can suggest that a kind of a complex of fixed stoichiometry is formed in the binary films. However, if this interpretation is true, a new kind of phase separation is here possible, that is the separation of the terpene–CL complex from the terpene-rich phase. The validity of such hypothesis can be verified by BAM visualization of the investigated monolayers.

Regarding the C_S^{-1}max–X(terpene) plots important differences can be observed between the systems with BAc and those with Ola and Urs. Moreover, these plots differentiate the bacterial cardiolipin from the two eukaryotic species. In systems with Ola and Urs the maximal value of compression modulus grows linearly with X(terpene) with the exception of the highest terpene proportion which has a significant

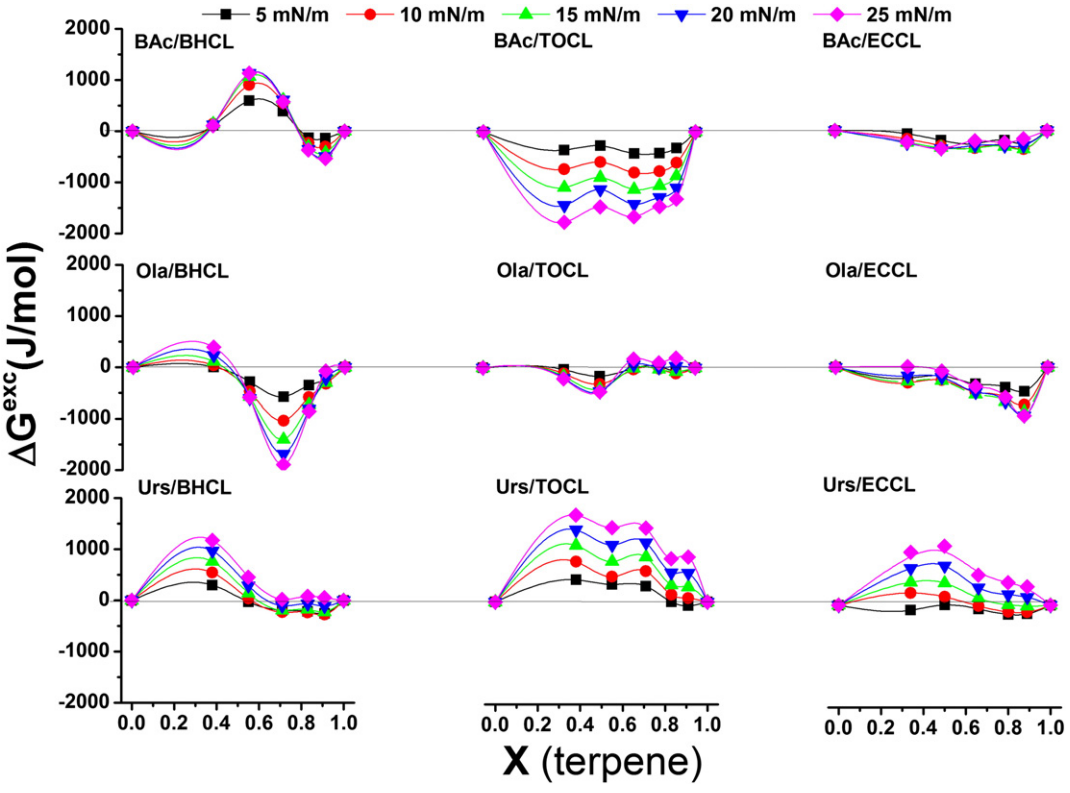

Fig. 2. ΔG^{exc}–X(terpene) dependences for the systems containing cardiolipins.

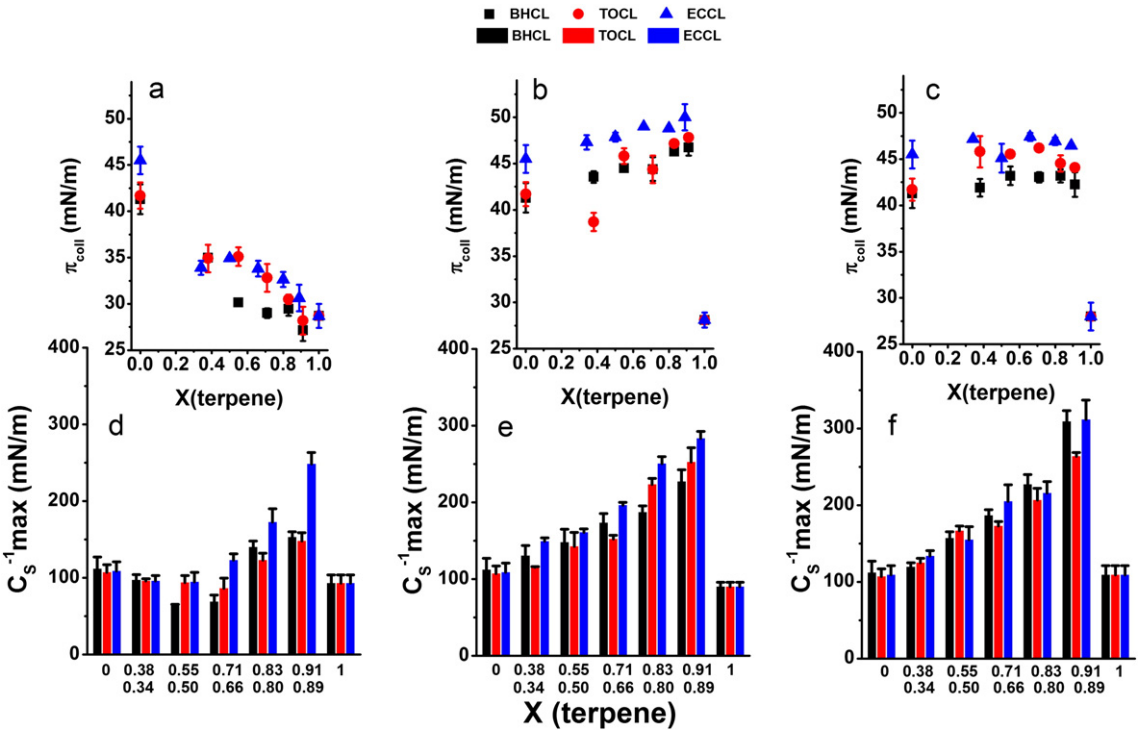

Fig. 3. Collapse pressures–X(terpene) dependences for the systems with: a) BAc, b) Ola, and c) Urs. Maximal compression modulus values vs X(terpene) dependences for the systems with: d) BAc, e) Ola, and f) Urs. X axis in panels d–f — upper labels for systems with BHCL and TOCL and lower for systems with ECCL.

positive deviation from the linear trend. On the contrary, in the systems with BAc the maximal value of C_S^{-1} decreases with growing X(BAc) till the mole ratio of 0.71. For the ratios of 0.83 and 0.91 an increase in film condensation is observed, which is much higher in the system with ECCL than in the systems with eukaryotic CLs.

All the monolayers within the 9 discussed systems here were visualized by BAM upon their compression. It turned out that most of the monolayers were homogenous similarly to the one-component cardiolipin films. Homogenous BAM images were observed in some systems even at the highest X(terpene) of 0.91. The only systems for which at some X(terpene) 2D and 3D domains were visible in BAM images were BAc/BHCL and Ola/ECCL. The representative images are shown in Fig. 4.

From the three systems containing BAc and CLs, positive ΔG^{exc} values are observed only in the system BAc/BHCL, so in this system immiscibility of the components is most probable. This assumption is corroborated by BAM images at high BAc proportion. For X(BAc) = 0.83 and 0.91 at π exceeding 10 mN/m the monolayers were heterogeneous proving the co-existence of separated phases. At the panels a–c large condense domains coexist with small circular structures. Moreover, some of the domains are very bright which suggests that they are rather 3D crystallites. At lower X(BAc) the monolayers were completely homogenous, so it can be supposed that BAc and BHCL were miscible even though the ΔG^{exc} acquired positive values. At the highest X(BAc) phase separation is observed; however, a question of what was the composition of the separating phases can be asked. The large condense islets visible in

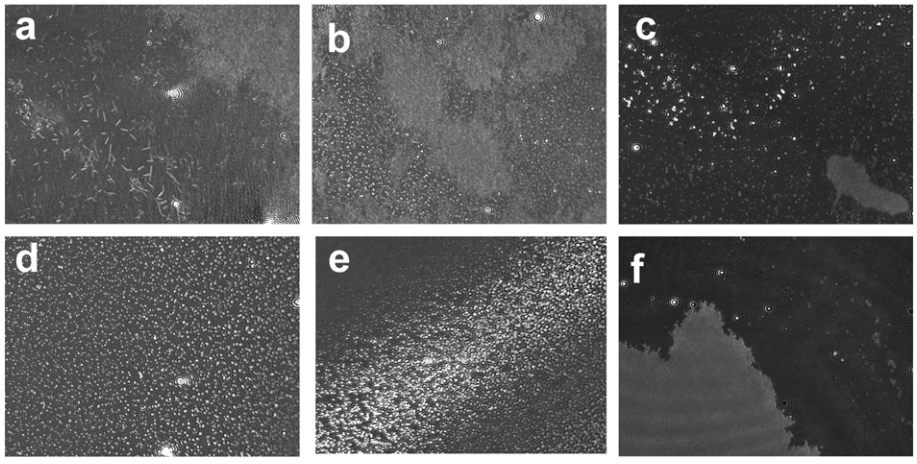

Fig. 4. Representative BAM images for the systems: a–c) BAc/BHCL and d–f) Ola/ECCL: a) X(BAc) = 0.83, π = 11.8 mN/m, b) X(BAc) = 0.83, π = 14.3 mN/m; c) X(BAc) = 0.91, π = 15 mN/m, d) X(Ola) = 0.50, π = 14.2 mN/m e) X(Ola) = 0.66, π = 21 mN/m, and f) X(Ola) = 0.89, π = 6.1 mN/m.

panels a–c of Fig. 4 are in some aspects similar to the domains observed for one-component BAc monolayers (Fig. 1). Thus, it is probable that the condensed islets are composed solely of BAc molecules oriented uprightly at the interface, whereas the numerous small domains are a two component phase containing both BAc and the remaining BHCL. Interesting phase separations were observed in the system Ola/ECCL (panels d–e). Upon the compression of the binary films at a surface pressure of ca. 15–20 mN/m numerous bright points appeared in the BAM photos. Such behavior was not observed only at the lowest X(Ola) of 0.34. Such bright points are usually interpreted as the manifestation of 3D phase expulsion from the monolayer. One-component ECCL monolayers had the liquid-expanded character and such bright domains were not observed for them, so in the case of the mixed Ola/ECCL films it is probable that the aggregates are formed by the Ola molecules. It is interesting that the expulsion of Ola molecules is not manifested in the course of the π–A isotherms and consequently in the C_S^{-1}–π curves (the dependences are presented in Supplementary materials). Similar phenomena were observed in the artificial membranes composed of membrane phospholipids and cholesterol [38]. There the expelled cholesterol molecules were treated as excess — a certain stoichiometry of the cholesterol–phospholipid domains was assumed and the domains were observed when the proportion of cholesterol was too high.

3.2. Interactions of triterpene acids with phosphatidylglycerols

Similar studies have been performed for 9 systems containing phosphatidylglycerols correlated with the investigated cardiolipins as it was described in the Experimental section. The π–A isotherms registered for these systems and the related C_S^{-1}–π plots are presented in Supplementary materials. Here we present the results of the thermodynamic analysis in the form of ΔG^{exc}–X(terpene) plots (Fig. 5).

Similarly to the systems with CLs also here BAc can be considered as the terpene discriminating over the eukaryotic PGs as the ΔG^{exc} values in the system with DLPG are significantly negative, whereas in the system with DOPG positive for lower BAc ratios of 0.34 and 0.5 and close to 0 for higher ratios. Ola does not discriminate over DLPG and DOPG as the ΔG^{exc}–X(Ola) dependences are similar for both PGs — ΔG^{exc} has positive sign for lower X(Ola) and negative for higher X(Ola). The results for the system Ola/ECPG differ from those with eukaryotic PGs, as here ΔG^{exc} values are close to 0 regardless of the Ola ratio. Urs also does not discriminate over eukaryotic PGs as for both investigated compounds here ΔG^{exc} acquires positive sign. On the other hand, it can be stated that this triterpene acid discriminates over prokaryotic and eukaryotic PGs as in the system Urs/ECPG ΔG^{exc} values are slightly negative. The differences between the systems with CLs and PGs should also be underlined. For all systems containing Urs and CLs the sign of ΔG^{exc} was positive and the values at higher surface pressures exceeded 1000 J/mol. The main difference here is the negative sign of the ΔG^{exc}–X(Urs) dependence in the system Urs/ECPG. Important differences can be also observed between the systems with BAc. For example the sign of ΔG^{exc} for lower X(BAc) ratios was positive in the system BAc/BHCL, whereas in the system BAc/DLPG it is negative for all mole ratios. In the systems with Ola discernable differences can be observed between the systems Ola/TOCL and Ola/DOPG. In the former case ΔG^{exc} is close to 0 for all Ola proportions, whereas in the latter it is positive for X(Ola) < 0.66.

Similarly to the systems with CLs, we also chose π_{coll}–X(terpene) and C_S^{-1}max–X(terpene) dependences for the illustration of the effect of the alterations in component proportions on the monolayer properties for the systems with PGs (Fig. 6).

Regarding the π_{coll}–X(terpene) plots the trends observed here for the systems with BAc and Ola are identical as for the systems with CLs. The collapse pressure falls linearly with X(terpene) in the former case and remains on a constant level regardless of X(terpene) in the

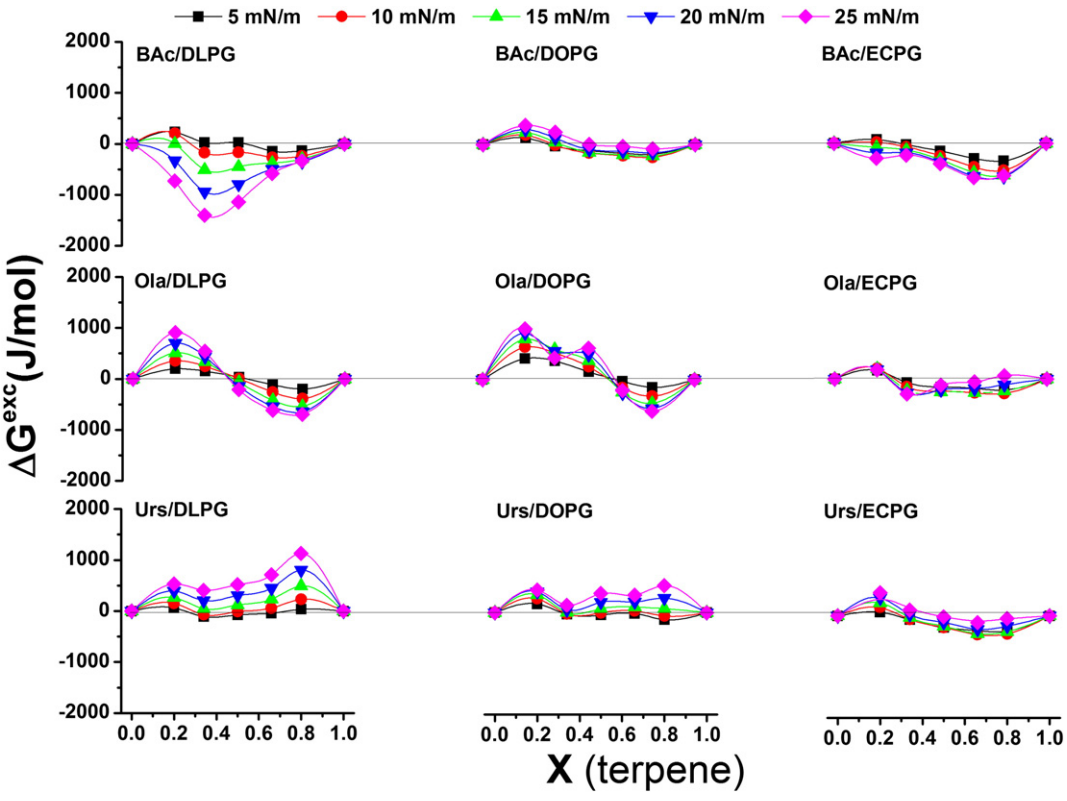

Fig. 5. ΔG^{exc}–X(terpene) dependences for the systems containing phosphatidylglycerols.

latter. Some differences can be noticed between the systems containing Urs. A constant value of π_{coll} is observed in the systems with TOCL and ECCL similarly to the systems with CLs. In contrast, the fall of collapse pressure with X(terpene) can be observed in the system Urs/BHCL, whereas in the analogous system with CLs (Urs/ECCL) the collapse pressure remained at a constant level regardless of X(Urs).

Regarding the C_S^{-1}max–X(terpene) dependences much larger differences can be observed between ECPG and the eukaryotic PGs, as it was in the systems with CLs. Generally, the monolayers containing ECPG are significantly more condensed than those containing eukaryotic PGs at the same X(terpene). These differences are most profound between the systems with Ola, where the C_S^{-1}max values at a given X(terpene) are approximately two times higher than those in the systems Ola/DLPG and Ola/DOPG. Special attention should be paid regarding the very high values of C_S^{-1}max observed at X(terpene) = 0.66 and 0.8 in the systems Ola/ECPG and Urs/ECPG. The C_S^{-1} values exceed the limiting value of 250 mN/m [39], thus, according to the classical description of the physical states of 2D films, it can be stated that the state of these monolayers is solid.

All the monolayers within the 9 systems containing PGs were visualized by BAM upon their compression. Similarly to the systems with CLs most of the films were homogenous regardless of surface pressure value. In the systems BAc/DLPG, BAc/ECPG and Ola/ECPG at some component proportions condense domains were visible. However, the observed textures were not conclusive for the interpretation of the PTA–PG interactions; thus the selected BAM images for the mentioned systems together with their description are presented in Supplementary materials.

4. Discussion

In our studies we selected the thermodynamic criterion for the discussion of the mutual interaction of the PTAs and anionic phospholipids in the model environment. The negative sign of ΔG^{exc} indicates that two different molecules in a binary film attract themselves more strongly than those identical molecules in one-component monolayers. On the contrary, the positive sign of ΔG^{exc} indicates that the interactions between two different molecules are not energetically favorable as referred to pure one-component monolayers [34]. There appears a problem of how to transfer the trends observed for the investigated artificial systems to real biomembranes, and especially how to interpret the information hidden in the ΔG^{exc}–X(terpene) plots. We expect that PTA molecules acting as an effective drug should exert destructive effects on the organization of the bacterial or mitochondrial membranes. As destructive for membranes we can understand significant changes in membrane fluidity and changes in permeation. Both phenomena can be triggered when additional 2D or 3D lipid domains separate within the CL-rich regions or when triterpene molecules incorporated between CL molecules disturb their packing. For all such cases the terpene–CL interactions would be energetically unfavorable and ΔG^{exc} values would be positive. Therefore, we should look for the systems were ΔG^{exc} values are positive. In such systems the probability of the abovementioned phenomena is increased. Positive values can be found for all the systems with Urs, thus this PTA can be considered as the compound of choice. Urs exhibits high antibacterial activity, which was proved by different studies; however, these studies usually estimated Ola to have similar activity.

Our results show also significant differences between BAc and the other two PTAs. Such differences were also observed in the studies performed on cancer or bacterial cell lines as well as in-vivo on laboratory animals [8,16]. BAc turned out to be most effective as an anticancer drug but was not effective as bacteriocide [16]. Our results obtained on artificial model systems are in agreement with those observations. ΔG^{exc} is positive for most compositions in the system BAc/BHCL but close to 0 in the system BAc/ECCL. Thus, a question of what is the origin of the differences between BAc and the other two PTAs arises. As it was mentioned in the Introduction the three PTAs differ in the structure of the E ring and in its substitution. BAc has there a smaller pentacyclic

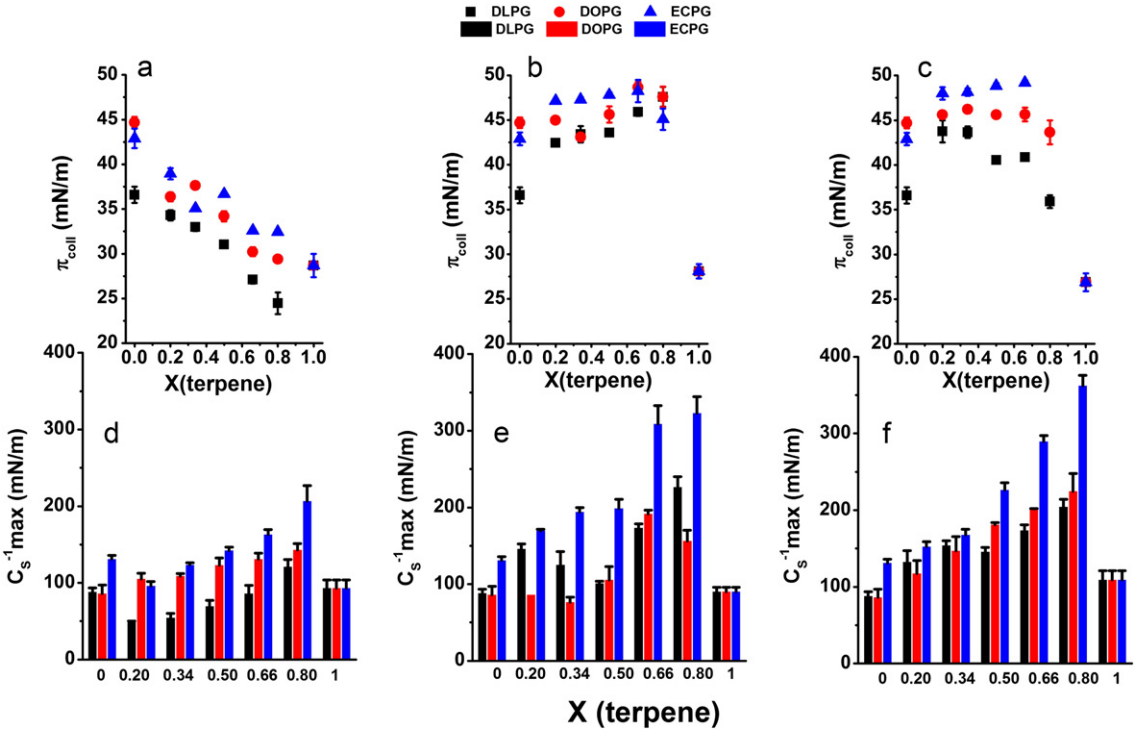

Fig. 6. Collapse pressures–X(terpene) dependences for the systems with: a) BAc, b) Ola, and c) Urs. Maximal compression modulus values vs X(terpene) dependences for the systems with: d) BAc, e) Ola, and f) Urs.

cyclopentane ring, whereas the other two have there cyclohexane. Moreover, BAc is structurally similar to hopane pentacyclic triterpenes [16] (structures in Supplementary materials). It can be of utmost importance because hopanoids are often present in bacterial membranes where they are hypothesized to play the same role as sterols in eukaryotic membranes [40,41]. The structural similarity of lupanes to hopanes may render these terpenes inactive when incorporated into bacterial membranes [16]. Writing about BAc it should be underlined that our results indicated that this terpene can discriminate over BHCL and TOCL. For BHCL ΔG^{exc} values were positive (or close to 0 for higher X(BAc)), whereas for TOCL the values of ΔG^{exc} were significantly negative. Moreover, the discussed problems here found also manifestation in BAM images. The monolayers in the system BAc/TOCL were homogenous regardless of X(BAc), whereas in the system BAc/BHCL at the highest X(BAc) of 0.83 and 0.91 condensed domains were visible. At these terpene proportions the separation of multiple small 3D domains was observed at ca. 15 mN/m. It was not the monolayer collapse as the π–A isotherm increased smoothly to much higher surface pressures. It seems that BAc molecules separated from the mixed film as multilayer crystallites. Similar phenomena were also observed in model multicomponent monolayers containing steroids [38]. Nonetheless, the presence of separated terpene-rich domains can here be crucial for the understanding of the mechanism of PTA action. PTAs were reported to generate reactive oxygen species (ROS) which can lead to cardiolipin peroxidation and the permeation of mitochondrial membrane [14,42]. Here we have BAc-rich domains which can be treated as catalytic centers on which ROS can be generated; however, these centers are in close proximity to cardiolipin molecules which can be damaged because of ROS appearance. The presence of small 3D domains was observed also in BAM images registered for the system Ola/ECCL at some X(Ola). Here a problem arises: taking into consideration ΔG^{exc} criterion Urs should be more destructive to bacterial membranes than Ola, but in the system Urs/ECCL all the monolayers were homogenous, regardless of X(Urs). However, in such discussion the scale problem should be signaled. The resolution of BAM is 2 μm, so the fact that a film is homogenous does not automatically exclude the possibility of phase separation in Langmuir monolayers. There can form microdomains rich in Urs in the systems containing this terpene, but if they are smaller than 2 μm, they are invisible in BAM images.

As it was mentioned at the beginning of the Results section, PTAs are specific bolaamphiphilic molecules in which the hydrophobic moiety is stiff and cannot be bent to achieve U-shaped conformation typical for multiple bolaamphiphiles at the water/air interface [35,37]. Thus, two different orientations of PTA molecules at the air water interface are possible — the upright with the –OH group in contact with water and the tilted with the –COOH group in water [35]. If the two conformations were present also in the binary mixtures the effective packing of the PTA and CL molecules would not be possible. Thus it is probable, that because of the PTA interaction with CLs one of the conformations is eliminated. Because at high X(terpene) higher C_S^{-1} values, often exceeding 250 mN/m, were observed it is probable that the tilted conformation of PTAs is eliminated and the molecules in binary mixtures acquire only the upright orientation. It is interesting that even at small proportion of CLs the tilted conformation of PTAs is eliminated — the monolayers are homogenous and the C_S^{-1} values are very high.

Regarding the results obtained for the systems with PGs the differences between the bacterial PG (ECPG) and the eukaryotic species should be underlined. The incorporation of Ola and Urs into ECPG monolayers affects their fluidity leading to a significant increase of the observed C_S^{-1} values, whereas for eukaryotic PGs such condensation is not observed. PGs are not recognized to be important components of mitochondrial membranes [43] but in *E. coli* membranes they constitute 20% of all phospholipids [32]. Therefore, interpreting the results obtained for the investigated model systems we can distinguish two different mechanisms of the PTA action on bacterial membranes. The incorporation of Urs into the CL-rich domains can trigger phase separation within them and by this phenomenon lead to their destruction. On the other hand the interaction of Ola and Urs with bacterial PGs can lead to a significant condensation of the bacterial membrane and by this disturb its function.

5. Conclusions

In our studies we applied Langmuir monolayers as versatile platforms for the investigations of the interactions between pentacyclic triterpene acids and anionic phospholipids from mitochondrial and bacterial membranes. We looked especially for the systems in which ΔG^{exc} had positive sign and significant values assuming that in such systems PTAs would exert the most destructive effect on CL and PG organization. The studies performed in the model environment indicated that Urs can be the most destructive agent, the incorporation of which can lead to the disintegration of CL-rich domains. However, this compound was not selective — the ΔG^{exc}–X(terpene) plots were similar for the three investigated cardiolipins. On the contrary, BAc exhibited high selectivity regarding its interactions with CLs. It turned out that mixing of BAc with TOCL, the main CL of human lymphoblasts, is energetically beneficial; whereas its interactions with BHCL — the main animal CL are energetically unfavorable. On the other hand, the model studies proved, that BAc can be non-active against bacterial cardiolipin. This finding was interpreted taking into consideration the structural similarity between BAc and hopanoids — pentacyclic terpenes occurring in bacterial membranes. For some of the investigated systems extrusions of small 3D domains were observed in BAM images. It was proposed that these multilayer nuclei are PTA-rich domains. The presence of such domains in the bacterial or mitochondrial membrane can lead to alterations of its structure and function. It is possible that such domains can become the centers of reactive oxygen species generation, as it was suggested in the scientific literature. For comparison reasons we performed also similar investigations on systems composed of the three PTAs and phosphatidylglycerols structurally correlated with the applied cardiolipins. These studies indicated important differences between the eukaryotic and bacterial PGs. These differences were especially visible in the significant increases of the monolayer condensation of the films composed of Urs or Ola and ECPG. The experiments performed on artificial model systems proved the direct interactions of PTAs with cardiolipins and bacterial phosphatidylglycerols; however, the character of the interactions still requires further elucidation, both on model systems and on living cell lines.

Acknowledgement

This project was financed by the National Science Centre (No. DEC-2012/05/B/ST5/00287).

The research was carried out with the equipment (UltraBAM) purchased thanks to the financial support of the European Regional Development Fund in the framework of the Polish Innovation Economy Operational Program (contract no. POIG.02.01.00-12-023/08).

Appendix A. Supplementary data

Supplementary data to this article can be found online at http://dx.doi.org/10.1016/j.bbamem.2014.05.027.

References

[1] S. Jager, H. Trojan, T. Kopp, M. Laszczyk, A. Scheffler, Pentacyclic triterpene distribution in various plants — rich sources for a new group of multi-potent plant extracts, Molecules 14 (2009) 2016–2031.
[2] J. Liu, Oleanolic acid and ursolic acid: research perspectives, J. Ethnopharmacol. 100 (2005) 92–94.
[3] T.G. Tolstikova, I.V. Sorokina, G.A. Tolstikov, A.G. Tolstikov, O.B. Flekhter, Biological activity and pharmacological prospects of lupane terpenoids: I. Natural lupane derivatives, Russ. J. Bioorg. Chem. 32 (2006) 37–49.
[4] D.W. Nes, E. Heftmann, A comparison of triterpenoids with steroids as membrane components, J. Nat. Prod. 44 (1981) 377.

[5] M.N. Laszczyk, Pentacyclic triterpenes of the lupane, oleanane and ursane group as tools in cancer therapy, Planta Med. 75 (2009) 1549–1560.
[6] J.M.R. Patlolla, C.V. Rao, Triterpenoids for cancer prevention and treatment: current status and future prospects, Curr. Pharm. Biotechnol. 13 (2012) 147–155.
[7] R.Y. Kuo, K. Qiuan, S.L. Morris-Natschke, K.H. Lee, Plant-derived triterpenoids and analogues as antitumor and anti-HIV agents, Nat. Prod. Rep. 26 (2009) 1321–1344.
[8] S. Fulda, Betulinic acid: a natural product with anticancer activity, Mol. Nutr. Res 53 (2009) 140–146.
[9] M.K. Shanmugam, X. Dai, A.P. Kumar, B.K.H. Tan, G. Sethi, A. Bishayee, Ursolic acid in cancer prevention and treatment: molecular targets, pharmacokinetics and clinical studies, Biochem. Pharmacol. 85 (2013) 1579–1587.
[10] S. Fulda, C. Scaffidi, S.A. Susin, P.H. Krammer, G. Kroemer, M.E. Peter, K.M. Debatin, Activation of mitochondria and release of mitochondrial apoptogenic factors by betulinic acid, J. Biol. Chem. 273 (1998) 33942–33948.
[11] D.V.R. Gopal, A.A. Narkar, Y. Badrinath, K.P. Mishra, D.S. Joshi, Betulinic acid induces apoptosis in human chronic myelogenous leukemia (CML) cell line K-562 without altering the levels of Bcr-Abl, Toxicol. Lett. 155 (2005) 343–351.
[12] P.O. Harmand, R.J. Duvall, C. Delage, A. Simon, Ursolic acid induces apoptosis through mitochondrial intrinsic pathway and caspase-3 activation in M4Beu melanoma cells, Int. J. Cancer 114 (2005) 1–11.
[13] M.H. Shyu, T.C. Kao, G.C. Yen, Oleanolic acid and ursolic acid induce apoptosis in HuH7 human hepatocellular carcinoma cells through a mitochondrial-dependent pathway and downregulation of XIAP, J. Agric. Food Chem. 58 (2010) 6110–6118.
[14] I. Samudio, M. Konopleva, H. Pelicano, P. Huang, O. Frolova, W. Bornmann, Y. Ying, R. Evans, R. Contractor, M. Andreeff, A novel mechanism of action of methyl-2-cyano-3,12 dioxoolean-1,9 diene-28-oate: direct permeabilization of the inner mitochondrial membrane to inhibit electron transport and induce apoptosis, Mol. Pharmacol. 69 (2006) 1182–1193.
[15] K.I. Wolska, A.M. Grudniak, B. Fiecek, A. Kraczkiewicz-Dowjat, A. Kurek, Antibacterial activity of oleanolic and ursolic acids and their derivatives, Cent. Eur. J. Biol. 5 (2010) 543–553.
[16] S. Fontanay, M. Grare, J. Mayer, C. Finance, R.E. Duval, Ursolic, oleanolic and betulinic acids: antibacterial spectra and selectivity indexes, J. Ethnopharmacol. 120 (2008) 272–276.
[17] V. Kuete, S. Albert-Franco, K.O. Eyong, B. Ngameni, G.N. Folefoc, J.R. Nguemeving, J.G. Tangmouo, G.W. Fotso, J. Komguem, B.M.W. Ouahouo, J.M. Bolla, J. Chevalier, B.T. Ngadjui, A.E. Nkengfack, J.M. Pagcs, Antibacterial activity of some natural products against bacteria expressing a multidrug-resistant phenotype, Int. J. Antimicrob. Agents 37 (2011) 156–161.
[18] S.G. Kim, M.J. Kim, D. Jin, S.N. Park, E. Cho, M. Oliveira Freire, S.J. Jang, J.K. Kook, Antimicrobial effect of ursolic acid and oleanolic acid against methicillin-resistant *Staphylococcus aureus*, Korean J. Microbiol. 48 (2012) 212–215.
[19] R.H. Cichewicz, S.A. Kouzi, Chemistry, biological activity, and chemotherapeutic potential of betulinic acid for the prevention and treatment of cancer and HIV infection, Med. Res. Rev. 24 (2004) 90–114.
[20] C. Aiken, C.H. Chen, Betulinic acid derivatives as HIV-1 antivirals, Trends Mol. Med. 11 (2005) 31–36.
[21] Y. Ikeda, A. Murakami, H. Ohigashi, Ursolic acid: an anti- and pro-inflammatory triterpenoid, Nutr. Food Res. 52 (2008) 26–42.
[22] C.L. de Melo, M.G.R. Queiroz, A.C.V. Arruda Filho, A.M. Rodrigues, D.F. de Sousa, J.G.L. Almeida, O.D.L. Pessoa, E.R. Sillveira, D.B. Menezes, T.S. Melo, F.A. Santos, V.S. Rao, Betulinic acid, a natural pentacyclic triterpenoid, prevents abdominal fat accumulation in mice fed a high-fat diet, J. Agric. Food Chem. 57 (2009) 8776–8781.
[23] K.Y. Yoo, S.Y. Park, Terpenoids as potential anti-Alzheimer's disease therapeutics, Molecules 17 (2012) 3524–3538.
[24] R. Xu, G.C. Fazio, S.P.T. Matsuda, On the origins of triterpenoid skeletal diversity, Phytochem. 65 (2004) 261–291.
[25] H.L. Ziegler, H. Franzyk, M. Sairafianpour, M. Tabatabai, M.D. Tehrani, K. Bagherzadeh, H. Hagerstrand, D. Staerk, J.W. Jaroszewski, Erythrocyte membrane modifying agents and the inhibition of *Plasmodium falciparum* growth: structure–activity relationships for betulinic acid analogues, Bioorg. Med. Chem. 12 (2004) 119–127.
[26] J. Prades, O. Vogler, R. Alemany, M. Gomez-Florit, S.S. Funari, V. Ruiz-Gutierrez, F. Barcelo, Plant pentacyclic triterpenic acids as modulators of lipid membrane physical properties, Biochim. Biophys. Acta Biomembr. 1808 (2011) 752–760.
[27] S.D. Dyall, M.T. Brown, P.J. Johnson, Ancient invasions: from endosymbionts to organelles, Science 309 (2004) 253–257.
[28] M. Schlame, D. Rua, M.M.L. Greenberg, The biosynthesis and functional role of cardiolipin, Prog. Lipid Res. 39 (2000) 257–288.
[29] R.H. Houtkooper, F.M. Vaz, Cardiolipin, the heart of mitochondrial metabolism, Cell. Mol. Life Sci. 65 (2008) 2493–2506.
[30] E. Mileykovskaya, W. Dowhan, Cardiolipin membrane domains in prokaryotes and eukaryotes, Biochim. Biophys. Acta Biomembr. 1788 (2009) 2084–2091.
[31] K. Ariga, J.P. Hill, Monolayers at air–water interfaces: from origins-of-life to nanotechnology, Chem. Rec. 11 (2011) 199–211.
[32] R.F. Epand, P.B. Savage, R.M. Epand, Bacterial lipid composition and the antimicrobial efficacy of cationic steroid compounds (Ceragenins), Biochim. Biophys. Acta 1768 (2007) 2500–2509.
[33] www.avantipolarlipids.com.
[34] I.S. Costin, G.T. Barnes, Two-component monolayers II. Surface pressure–area relations for the octadecanol–docosyl sulphate system, J. Colloid Interface Sci. 51 (1975) 106.
[35] M. Broniatowski, M. Flasiński, P. Wydro, Lupane-type pentacyclic triterpenes in Langmuir monolayers: a synchrotron radiation scattering study, Langmuir 28 (2012) 5201–5210.
[36] G. Brezesinski, D. Vollhardt, Model studies of the interfacial ordering of oleanolic acid in the cuticula, ChemPhysChem 9 (2008) 1670–1672.
[37] N. Nuraje, H. Bai, K. Su, Bolaamphiphilic molecules: assembly and applications, Prog. Polym. Sci. 38 (2013) 302–343.
[38] K. Hąc-Wydro, P. Dynarowicz-Łątka, Externalization of phosphatidylserine from inner to outer layer may alter the effect of plant sterols on human erythrocyte membrane — the Langmuir monolayer studies, Biochim. Biophys. Acta Biomembr. 1818 (2013) 2184–2191.
[39] J.T. Davies, E.K. Rideal, Interfacial Phenomena, 2nd ed. Academic Press, New York, 1963.
[40] J.P. Saenz, Hopanoid enrichment in a detergent resistant membrane fraction of *Crocosphaera watsonii*: implications for bacterial lipid raft formation, Org. Geochem. 41 (2010) 853–856.
[41] P.V. Welander, R.C. Hunter, L. Zhang, A.L. Sessions, R.E. Summons, D.K. Newman, Hopanoids play a role in membrane integrity and pH homeostasis in *Rhodopseudomonas palustris* TIE-1, J. Bacteriol. 191 (2009) 6145–6156.
[42] J. Wang, L. Liu, H. Qiu, X. Zhang, W. Guo, W. Chen, Y. Tian, L. Fun, D. Shi, J. Cheng, W. Huang, M. Deng, Ursolic acid simultaneously targets multiple signaling pathways to suppress proliferation and induce apoptosis in colon cancer cells, PLoS One 8 (2013) e63872.
[43] F. Cronier, A. Patenaude, R.C. Gaudreault, M. Auger, Membrane composition modulates the interaction between a new class of antineoplastic agents deriving from aromatic 2-chloroethylureas and lipid bilayers: a solid-state NMR study, Chem. Phys. Lipids 146 (2007) 125–135.